Inorganic Chemistry
Article

Inorg. Chem. **2009**, *48*, 9147–9154 **9147**
DOI: 10.1021/ic9008653

Investigation of the New P′3-$Na_{0.60}VO_2$ Phase: Structural and Physical Properties

Olivier Szajwaj,[†] Etienne Gaudin,[†] François Weill,[†,‡] Jacques Darriet,*[,†] and Claude Delmas[†]

[†]*CNRS, Université de Bordeaux, ICMCB, 87 avenue du Dr. A. Schweitzer, 33608 Pessac Cedex, France, and* [‡]*Université de Bordeaux 1, CREMEM, Talence F-33405, France*

Received May 5, 2009

A new layered phase $Na_{0.60}VO_2$ was synthesized by chemical deintercalation of sodium from the pristine compound O3-$NaVO_2$. The $Na_{0.60}VO_2$ compound exhibits a distorted P′3-type oxygen stacking (AABBCC) with an average monoclinic unit cell containing $a = 4.9862(14)$ Å, $b = 2.8708(8)$ Å, $c = 5.917(2)$ Å, and $\beta = 104.36(3)°$. A modulated structure was observed by transmission electron microscopy and X-ray diffraction (XRD) measurements. Indexation of the XRD pattern was achieved by using the **q** vector equal to $0.44\boldsymbol{b}^*$, and the 4D superspace group $C2/m$ (0 β 0) s0 was then deduced. The specific heat measurement showed a strong correlated system with a γ value of around 20 $mJ \cdot mol^{-1} \cdot K^{-2}$. The electrical conductivity shows a semiconductor-like behavior with an activation energy of 0.52 eV. A paramagnetic behavior of the susceptibility is observed below room temperature with a Curie constant equal to $C = 0.076$ $emu \cdot K^{-1} \cdot mol^{-1} \cdot Oe^{-1}$. To explain this small value, a model of pseudotriangular clusters of vanadium with a random distribution of V^{3+} and V^{4+} was considered.

Introduction

The layered Na_xMO_2 oxides (M = 3d configuration ion) have been studied since the 1970s from the crystal chemistry point of view[1−4] and in the earlier 1980s as positive electrodes of sodium batteries in relation to their physical properties: electronic conductivity and thermoelectric power.[5−8] More recently, Terasaki et al.[9] discovered that the $Na_{0.50}CoO_2$ phase exhibits a high ZT value, which makes this material a potential candidate for thermoelectric applications, while Takada et al.[10] reported on the superconductivity of the $Na_{0.35}CoO_2 \cdot yH_2O$ phase. These two studies motivated a huge number of laboratories to revisit these materials in order to try to understand the relationship between the structure and the electronic properties of these materials. The peculiar interest of cobalt-layered phases results from the interaction between the Na^+ ion distribution in the interslab space and the electronic distribution (charge ordering) in the CoO_2 plane, which, in a first approximation, exhibits metallic properties.

The layered Na_xCoO_2 phases exhibit a wide variety of structures depending on the packing along the hexagonal c_h axes and x values. Depending on the Na/Co ratio or the synthesis method (temperature, solid-state chemistry, intercalation chemistry, etc.), each packing exhibits a composition range, which has overlapping values. Therefore, it is very confusing to use only the composition to design a given material. In order to clarify this situation, Delmas et al.[3] proposed a nomenclature to describe in a general way all of the existing phases of the A_xMO_2 formula (A = alkali ions). This nomenclature is based on the alkali ion surroundings (the letter) and the stacking along the c_h axis. The sodium ion may adopt oxygen octahedral (O), prismatic (P), or tetrahedral (T) surroundings, and the stacking consists of one (1), two (2), or three (3) layers along the c_h axis. Delmas et al.[5] were the first to observe the sodium ratio influence on the structural packing and then on the physical properties of the material obtained by intercalation chemistry. Various structural distortions can exist and are named, for instance, P′3 (monoclinic unit cell) in reference to P3 (hexagonal unit cell). Recently, because of interest in the interpretation of the properties of Na_xCoO_2, some structural characterizations have been performed to highlight a possible ordering of sodium and its influence on the properties. The P2-Na_xCoO_2 ($x \in [0.3, 0.7]$) compounds have been widely studied because of their physical properties, and various superstructures have been

*Corresponding author. Tel: + 33 5 40 00 62 59. Fax: + 33 5 40 00 27 61. E-mail: darriet@icmcb-bordeaux.cnrs.fr.

(1) Parant, J. P.; Olazcuaga, R.; Devalette, M.; Fouassier, C.; Hagenmuller, P. *J. Solid State Chem.* **1971**, *3*, 1.
(2) Jansen, M.; Hoppe, R. *Z. Anorg. Allg. Chem.* **1974**, *408*, 97.
(3) Delmas, C.; Fouassier, C.; Hagenmuller, P. *Physica B* **1980**, *99*, 81.
(4) Delmas, C.; Braconnier, J. J.; Fouassier, C.; Hagenmuller, P. *Z. Naturforsch.* **1981**, *36b*, 1368.
(5) Delmas, C.; Braconnier, J. J.; Fouassier, C.; Hagenmuller, P. *Solid State Ionics* **1981**, *3/4*, 165.
(6) Braconnier, J. J.; Delmas, C.; Hagenmuller, P. *Mater. Res. Bull.* **1982**, *17*, 993.
(7) Miyazaki, M.; Kikkawa, S.; Koizumi, M. *Synth. Met.* **1983**, *6*, 211.
(8) Molenda, J.; Delmas, C.; Hagenmuller, P. *Solid State Ionics* **1983**, *9/10*, 431.
(9) Terasaki, I.; Sasago, Y.; Uchinokura, K. *Phys. Rev. B* **1997**, *56*, R12685.
(10) Takada, K.; Sakurai, H.; Muromachi, E. T.; Izumi, I.; Dilanian, R. A.; Sasaki, T. A. *Nature* (*London*) **2003**, *422*, 53.

Published on Web 09/08/2009

observed.[11−20] Finally, Viciu et al.[21] have focused on the influence of the sodium content on the structural patterns of P′3-, O3-, and O′3-polytype Na_xCoO_2 phases ($0.3 \leq x \leq 0.92$). The only modulated phase evidenced is O′3-$Na_{0.75}CoO_2$, with a 4D modulation and $\mathbf{q} = 0.33\boldsymbol{a}^* - 0.247\boldsymbol{c}^*$.

In our laboratory, a study of the Na_xVO_2 ($x \leq 1$) system was recently carried out because interesting electronic properties could be expected for the partially deintercalated phases. The structure of $NaVO_2$ was first reported by Rüdorff and Becker in 1955.[22] The first study of the Na_xVO_2 system was performed by Barker and Hooper, who tried to synthesize $NaVO_2$ by the reaction of liquid sodium on VO_2.[23] This reaction was difficult to optimize, and they always obtained $NaVO_2$ mixed with impurities that seemed to be the Na_xVO_2 partially deintercalated phases. Similar results were obtained in 1988 by Chamberland and Porter, who claimed to obtain two varieties for $NaVO_2$: a high-temperature (200 °C) one with rhombohedral symmetry and a room temperature one with a lower symmetry.[24] In fact, it seems that at room temperature they obtained a mixture of the $NaVO_2$ rhombohedral phase with a partially deintercalated phase and other impurities, which react at 200 °C to form rhombohedral $NaVO_2$. Very recently, Onoda published a very interesting structural and magnetic study on $NaVO_2$ and on a new P2-$Na_{0.70}VO_2$ phase.[25] Cava et al.[26] have recently investigated the structural and magnetic properties of $NaVO_2$ by a neutron diffraction experiment and have shown, in particular, that a structural and magnetic transition took place near $T = 94$ K related to an orbital ordering that retrieves the geometrical frustration.

In this paper, we report our results on $Na_{0.60}VO_2$ with the P′3-type stacking and an interpretation of its physical properties.

Experimental Section

Na_xVO_2 samples ($x \approx 0.60$) have been prepared in two steps. First, $NaVO_2$ samples have been synthesized in a gold crucible by chemical reduction of a $NaVO_3$ powder under a dihydrogen atmosphere at 800 °C for 8 h. $NaVO_3$ had been previously synthesized by the solid-state reaction of a stoichiometric mixture of Na_2CO_3 (purity above 99.9%) and V_2O_5 (purity above 99.9%) by heating it in a platinum crucible up to the melting point. Then, sodium's extraction from the $NaVO_2$ powder was carried out by use of iodine in acetonitrile with stirring for 1 day at room temperature. Then, the residual powder was washed with acetonitrile, filtered, and dried under vacuum. Ratios of Na/I varying from 0.30 to 0.42 were tested. The iodine titration of the solution, after the powder was removed, confirmed that a complete reaction was observed until Na/I reached 0.40. The synthesis of the $Na_{0.60}VO_2$ phase has been optimized for the ratio Na/I = 0.42. A thermal treatment of the powder at 200 °C under vacuum improves slightly the crystallinity of the powder. Inductively coupled plasma atomic emission spectrometry measurements have confirmed the sodium content equal to 0.60(1). Because it is well-known that the transition-metal−oxide layer MO_2 is perfectly stoichiometric, one can deduce the formal formula $Na^{+}_{0.60}V^{3+}_{0.60}V^{4+}_{0.40}O_2$.

Powder X-ray diffraction (PXRD) patterns have been recorded on a Panalitycal X'pert diffractometer operating with Cu Kα radiation ($\lambda_1 = 1.5406$ Å and $\lambda_2 = 1.5444$ Å) in the range $5° \leq 2\theta \leq 80°$. The powders were put in a specific airtight holder under dry argon to prevent any reaction with air moisture. The structural refinement of the PXRD data was done with *JANA2000* software.[27,28] The background was estimated by a Legendre function, and the peak shapes were described by a pseudo-Voigt function. Refinement of the peak asymmetry was performed using the Simpson parameter.

Electron diffraction has been carried out on a JEOL 2000FX microscope operating at an accelerating voltage of 200 kV and equipped with a doubled tilt specimen stage. A small amount of $Na_{0.60}VO_2$ was crushed in methanol and then deposited on a copper grid.

Magnetization measurements were performed using a superconducting quantum interference device (SQUID) magnetometer in the 2−300 K temperature range with applied fields of up to 50 kOe.

Heat capacity measurements were performed using a quasi-adiabatic heat pulse method (Nernst calorimeter). The powder samples were encapsulated in an aluminum foil under a dry argon atmosphere. The heat capacity of the aluminum foil was subtracted after measurement. The temperature range for the measurement was 4−200 K.

Electrical direct-current conductivity measurements were performed with a four-probe method in the 170−300 K range in a specific sample holder to prevent any reaction with air moisture.

Results and Discussion

Structural Characterization. From our experiments on Na_xCoO_2 phases,[6] in some cases several phases with very close compositions can exist; therefore, thermal treatment at moderate temperature is a good way to homogenize the sample. The same behavior is observed for $Na_{0.60}VO_2$, and only thermal treatment at 200 °C led us to obtain a single phase. Powder patterns before and after thermal treatment are shown in Figure 1. The whole powder pattern of $Na_{0.60}VO_2$ shown in Figure 2

(11) Foo, M. L.; Wang, Y.; Watauchi, S.; Zandbergen, H. W.; He, T.; Cava, R. J.; Ong, N. P. *Phys. Rev. Lett.* **2004**, *92*, 247001.
(12) Shi, Y. G.; Yang, H. X.; Huang, H.; Liu, X.; Li, J. Q. *Phys. Rev. B* **2006**, *73*, 094505.
(13) Yang, H. X.; Shi, Y. G.; Nie, C. J.; Wu, D.; Yang, L. X.; Dong, C.; Yu, H. C.; Zhang, H. R.; Jin, C. Q.; Li, J. Q. *Mater. Chem. Phys.* **2005**, *94*, 119.
(14) Qian, D.; Wray, L.; Hsieh, D.; Wu, D.; Luo, J. L.; Wang, N. L.; Kuprin, A.; Fedorov, A.; Cava, R. J.; Viciu, L.; Hasan, M. Z. *Phys. Rev. Lett.* **2006**, *96*, 046407.
(15) Onoda, M.; Ikeda, T. *J. Phys.: Condens. Matter* **2007**, *19*, 186213.
(16) Huang, Q.; Khaykovich, B.; Chou, F. C.; Cho, J. H.; Lynn, J. W.; Lee, Y. S. *Phys. Rev. B* **2004**, *70*, 134115.
(17) Huang, Q.; Foo, M. L.; Lynn, J. W.; Zandbergen, H. W.; Lawes, G.; Wang, Y.; Toby, B. H.; Ramirez, A. P.; Ong, N. P.; Cava, R. J. *J. Phys.: Condens. Matter* **2004**, *16*, 5803.
(18) Zandbergen, H. W.; Foo, M.; Xu, Q.; Kumar, V.; Cava, R. J. *Phys. Rev. B* **2004**, *70*, 024101.
(19) Yang, H. X.; Nie, C. J.; Shi, Y. G.; Yu, H. C.; Ding, S.; Liu, Y. L.; Wu, D.; Wang, N. L.; Li, J. Q. *Solid State Commun.* **2005**, *134*, 403–408.
(20) Blangero, M.; Carlier, D.; Pollet, M.; Darriet, J.; Delmas, C.; Doumerc, J. P. *Phys. Rev. B* **2008**, *77*, 184116.
(21) Viciu, L.; Bos, J. W.; Zandbergen, H. W.; Huang, Q.; Foo, M. L.; Ishiwata, S.; Ramirez, A. P.; Lee, M.; Ong, N. P.; Cava, R. J. *Phys. Rev. B* **2006**, *73*, 174104.
(22) Rüdorff, W.; Becker, U. *Z. Naturforsch.* **1955**, *9b*, 613.
(23) Barker, M. G.; Hooper, A. J. *J. Chem. Soc., Dalton Trans.* **1973**, *15*, 1517.
(24) Chamberland, B. L.; Porter, S. K. *J. Solid State Chem.* **1988**, *73*, 398.
(25) Onoda, M. *J. Phys.: Condens. Matter* **2008**, *20*, 145205.
(26) McQueen, T. M.; Stephens, P. W.; Huang, Q.; Klimczuk, T.; Ronning, F.; Cava, R. J. *Phys. Rev. Lett.* **2008**, *101*, 166402.
(27) Petricek, V.; Dusek, M.; Palatinus, L. *Jana2000: The Crystallographic Computing System*; Institute of Physics: Praha, 2000.
(28) Altomare, A.; Burla, M. C.; Camalli, M.; Carrozzini, B.; Cascarano, G. L.; Giacovazzo, C.; Guagliardi, A.; Moliterni, A. G. G.; Polidori, G.; Rizzi, R. *J. Appl. Crystallogr.* **1999**, *32*, 339.

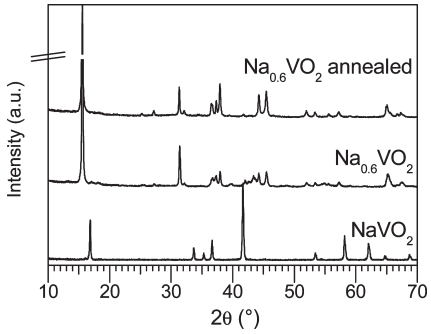

Figure 1. XRD pattern measured with Cu K$\alpha_{1,2}$radiation (λ_1 = 1.5406 Å and λ_2 = 1.5444 Å) at T = 293 K of $NaVO_2$, $NaVO_2$ after reaction with 0.2 mol of iodine corresponding to "$Na_{0.60}VO_2$", and $Na_{0.60}VO_2$ after annealing at 200 °C.

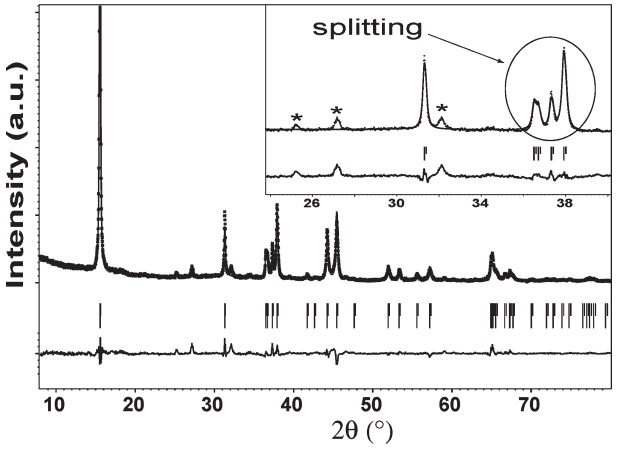

Figure 2. Rietveld refinement of the $Na_{0.60}VO_2$ PXRD pattern measured with Cu K$\alpha_{1,2}$ radiation (λ_1 = 1.5406 Å and λ_2 = 1.5444 Å) at T = 293 K. Vertical bars show the Bragg peak positions by considering the space group $C2/m$ and the cell parameters given in Table 1. The difference plot is shown at the bottom. The inset shows the splitting of the reflection, and the nonfitted peaks are marked with asterisks.

is similar to the Na_xCoO_2 (P′3) one, and this suggests an AABBCC oxygen packing with sodium ions in a trigonal prism.

Clearly, a monoclinic structural distortion takes place, as was previously reported for $Na_{0.60}CoO_2$.[3,20] This distortion is characterized by a splitting of some peaks, as shown in the inset of Figure 2. The ideal monoclinic cell is related to the hexagonal unit cell P3 with the following relation: $a_m = a_h - b_h$, $b_m = a_h + b_h$, and $c_m = (-a_h + b_h + c_h)/3$, where the subscripts m and h refer to the monoclinic and hexagonal cells, respectively. The refined unit cell parameters are a = 4.9862(14) Å, b = 2.8708(8) Å, c = 5.917(2) Å, and β = 104.36(3)° (Table 1). The usual space group $C2/m$ was observed for the homologous Na_xCoO_2 compounds fitted extinction conditions.[15,20,29] In line with the nomenclature that was used for P3, this structural type is named P′3 to emphasize the monoclinic distortion. This distortion is rather small because the ratio a/b = 1.737 is very close to $\sqrt{3}$. All peaks are indexed except for three small peaks observed within 25° < 2θ < 32° (inset of Figure 2).

Electron diffraction experiments were carried out in order to identify the origin of these additional weak

(29) Ono, Y.; Ishikawa, R.; Miyazaki, Y.; Ishii, Y.; Morii, Y.; Kajitani, T. *J. Solid State Chem.* **2002**, *166*, 177.

Table 1. Structural Parameters for $Na_{0.60}VO_2$

	$Na_{0.60}VO_2$[a]
polytype	P′3
space group	$C2/m$ (No. 12)
Z	2
cell parameters	
a (Å)	4.9862(14)
b (Å)	2.8708(8)
c (Å)	5.917(2)
β (deg)	104.36(3)
V (Å^3)	82.05(5)
a/b	1.737 ($\sqrt{3}$ = 1.732)

[a] Average structure.

peaks. Figure 3a shows an electron diffraction pattern for a crystallite of P′3-$Na_{0.60}VO_2$. The indexation of the main peaks was done by using the cell parameters a = 4.96 Å, b = 2.85 Å, c = 5.91 Å, and β = 104.3° and is in agreement with a C-centering of the unit cell. Along the b^* axis, weak spots are observed between the main spots. These weak spots cannot be simply indexed by considering a superstructure along the b^* axis. The interspacing corresponds to a fractional value of $\boldsymbol{b}^*$ associated with a **q** vector equal to 0.44$\boldsymbol{b}^*$ (Figure 3a). All peaks (main ones and satellites) are then fully indexed considering four indices ($hklm$) with m up to 3 (Figure 3a). Starting from the [−1 0 −1] zone axis (Figure 3a or 4a), a slight tilt of the crystal around the b^* direction leads to the disappearance of satellites of odd order (Figure 4b). This observation means a reflection condition due to the presence of a gliding symmetry element. The occurrence of the m = 1 and 3 satellites in Figure 3a or 4a is then due to a double diffraction phenomena. All of this information led us to propose the 4D superspace group $C2/m$ (0 β 0) s0.

Taking into account the superspace group $C2/m$ (0 β 0) s0, a full XRD pattern matching was done but was limited to the first-order satellite, as shown in Figure 5. All observed reflections are indexed with four integer indices ($hklm$) with respect to the previous main unit cell and with a unique **q** wave vector equal to 0.44(2)b^*. It can be noticed that the three most intense satellites observed in the XRD pattern are then perfectly indexed, as shown in Figure 5. However, the number of satellite reflections is too small to perform an accurate structural refinement of the modulated structure using the 4D superspace formalism. Therefore, the structural refinement was limited to the average structure. The average structure was investigated in a 3D approach with the space group $C2/m$ (Figure 2). The results are gathered in Table 2. A view of the structure is given in Figure 6. The vanadium atoms are located in an octahedral site with an average V−O distance of 1.94 Å (Table 3). The decrease of the V−O distances toward the one of $NaVO_2$ (≈2.05 Å) is consistent with the formal increase of the vanadium oxidation state, leading to a contraction of the $[VO_2]_n$ layers. For P′3-$Na_{0.60}VO_2$, the Na^+ ions have distorted trigonal-prismatic surroundings (Figure 6), as is observed for $Na_{0.62}CoO_2$, where Na^+ ions are shifted off the middle of the prismatic site in the xy plane. An explanation of the monoclinic distortion in $Na_{0.62}CoO_2$ has been proposed based on this sodium

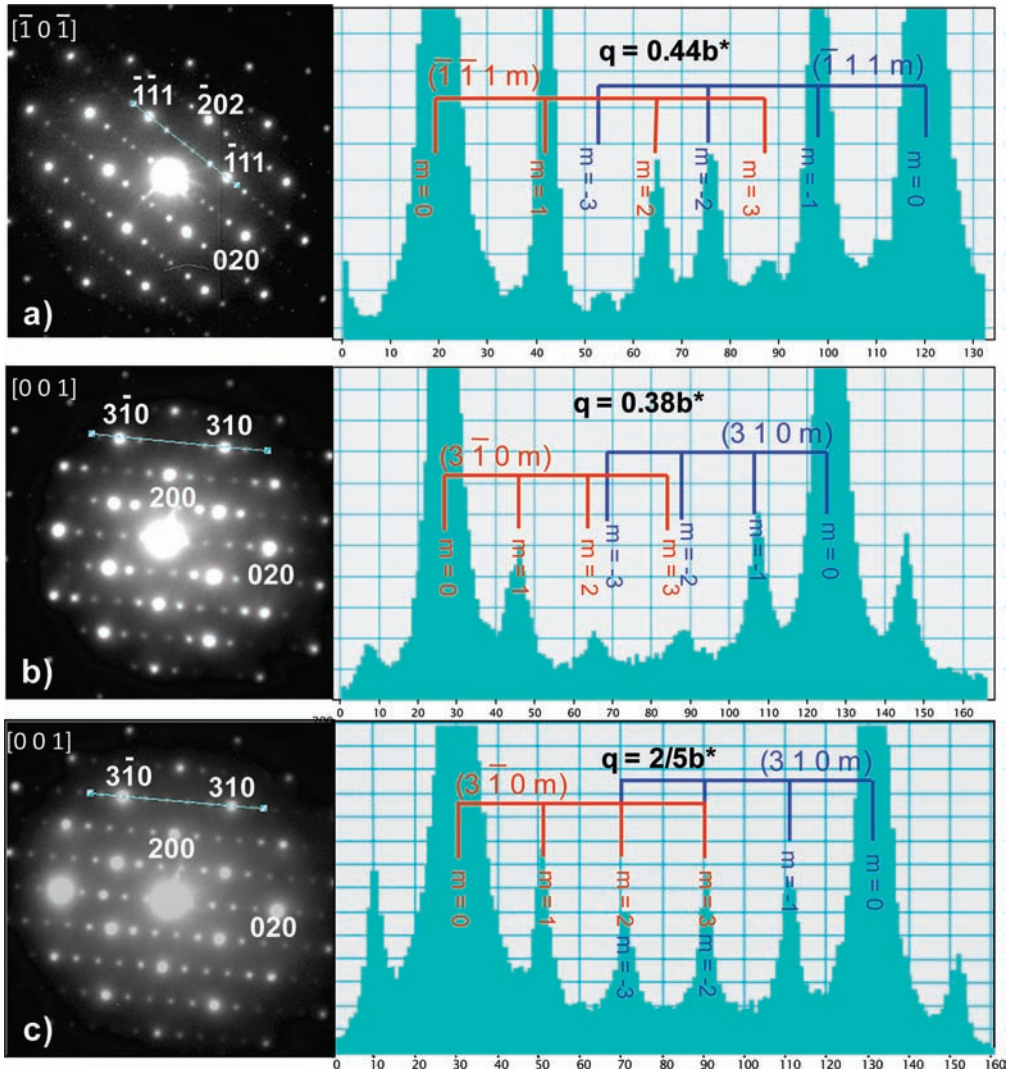

Figure 3. Electron diffraction pattern of three different crystals of P′3-$Na_{0.60}VO_2$. The right part of the figure represents the intensity evolution along the [0 1 0]* direction corresponding to the blue line in the pattern. The whole pattern can be indexed considering the cell parameters given in Table 1 and a vector **q** equal to (a) 0.44*b**, (b) 0.38*b**, and (c) 0.40*b**. The satellites are observed at least up to $m = 3$.

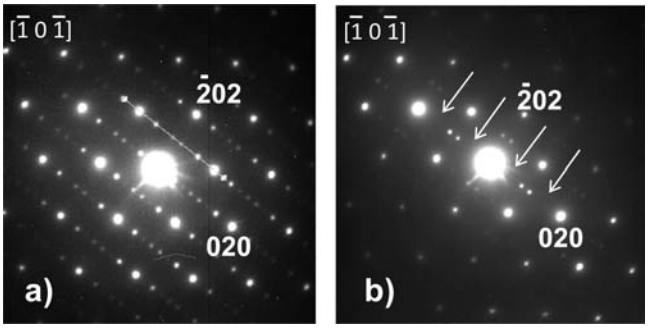

Figure 4. Electron diffraction pattern of (a) a crystal of P′3-$Na_{0.60}VO_2$ presenting a modulation along the b^* axis and (b) its tilt of a few degrees. The tilt makes the reflections $m = 1$ and 3 disappear, which is in agreement with the superspace group $C2/m$ (0 β 0) s0.

off-center displacement in order to minimize the coloumbic repulsion.[30] In our case, the structural model is only an average structure, and then it is not realistic to propose an explanation of the distortion based on the average atomic positions. In our case, the Na−O distances present two short average distances at 2.30 and 2.37 Å and four long average distances at 2 × 2.56 and 2 × 2.64 Å (Table 3). The Na−O distances are really greater in P′3-$Na_{0.60}VO_2$ than in $NaVO_2$ (≈2.36 Å), where the sodium atoms occupy an octahedral site. The large oxygen repulsions in the trigonal-prismatic environment imply an increase of the interslab distances in comparison to the cubic face center (cfc) oxygen packing of $NaVO_2$. Finally, more than the metal−O distance variation, we have to highlight that the sodium content must be less than 1 in order to observe realistic Na−Na distances. Indeed, for the P′3-Na_xVO_2 structure, an x value > 1 would imply Na−Na distances of 1.470(13) Å, which are absolutely unrealistic. At first sight, one can suppose that the modulation of the structure could be strongly related to the occupancy of the sodium site. It is therefore absolutely crucial to determine the structure on single crystals because a composite approach with two subsystems cannot be excluded, as was observed in

(30) Blangero, M.; Carlier, D.; Pollet, M.; Darriet, J.; Delmas, C.; Doumerc, J.-P. *Phys. Rev. B* **2008**, *77*, 184116.

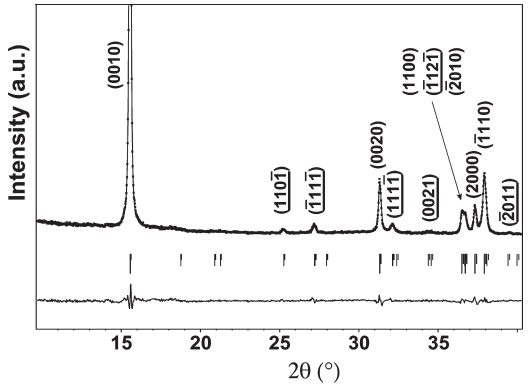

Figure 5. Full pattern matching of the PXRD pattern of $Na_{0.60}VO_2$ measured with Cu $K\alpha_{1,2}$ radiation (λ_1 = 1.5406 Å and λ_2 = 1.5444 Å) at T = 293 K. Vertical bars show the Bragg peak positions by considering the superspace group $C2/m$ (0 β 0) s0. The cell parameters are given in Table 1, and the vector $\mathbf{q} = 0.44\boldsymbol{b}^*$. The long black bars correspond to the main peaks, while the shortest gray bars correspond to the satellite. The difference plot is shown at the bottom. The indices of the first-order satellites are underlined.

Table 2. Crystallographic Data for P′3-$Na_{0.60}VO_2$ in the Space Group $C2/m$ (No. 12), with χ^2 = 1.32; R_{wp} = 9.25%; R_p = 6.67%

site	Wyckoff	occupancy	x	y	z	U_{iso} (Å^2)
V1	2a	1	0	0	0	0.027(4)
O1	4i	1	0.389(4)	0	0.174(3)	0.031(7)
Na1	4i	0.296(1)	0.781(8)	0	0.498(6)	0.03(2)

$Na_{1+x}CuO_2$ and $Cu_xV_4O_{11}$ materials.[31,32] If this is the case, the **q** vector should be directly related to the x sodium content.

Parts b and c of Figure 3 show the electron diffraction pattern of two other crystallites from the same preparation. Their electron diffraction patterns have been investigated because the previous crystal and two modulation vectors $\mathbf{q} = \beta\boldsymbol{b}^*$ are observed, with the β component equal to 0.38 and 0.40, respectively (Figure 3b,c). For the last crystal, the value of the β component is equal to $^2/_5$ and corresponds to a commensurate case. This explains the superposition of the satellite spots between the main spots in Figure 3c. A complete indexation with a 3D cell can be done by multiplying the c parameter by 5. The existence of different modulation vectors could be associated with variation of the sodium stoichiometry, as has been observed previously in $Na_{1+x}CuO_2$ (x = 1.58, 1.6, and 1.62).[31] In our case, the observed variation of the **q** vector could be explained by a loss of sodium during the sample preparation for the electron diffraction experiments where the powder is crushed in a polar solvent (methanol). A similar loss of sodium has already been observed in Na_xCoO_2 when the phase is crushed in methanol.[33] Another explanation for variation of the sodium content in our experiments could be that the crystals are electron-beam-sensitive, as was previously observed by Zandbergen et al. for a sample of $Na_{0.5}CoO_2$.[18]

(31) Rozier, P.; Lidin, S. *J. Solid State Chem.* **2003**, *172*, 319.
(32) van Smaalen, S.; Dinnebier, R.; Sofin, M.; Jansen, M. *Acta Crystallogr.* **2007**, *B63*, 17.
(33) Braconnier, J.; Thesis, University of Bordeaux, 1983.

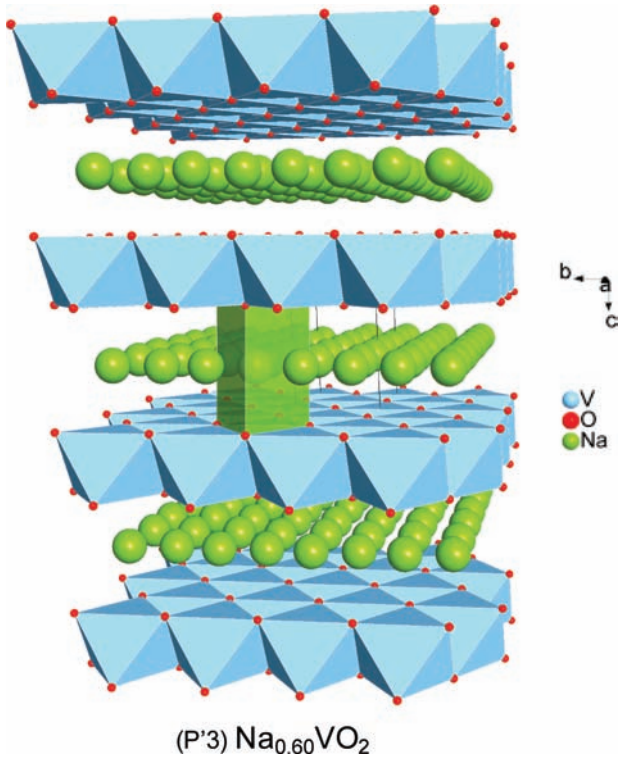

Figure 6. View of the structure of P′3-$Na_{0.60}VO_2$. All VO_6 octahedra and only one NaO_6 trigonal prism are drawn.

Table 3. Distances M−O (Å) for P′3-$Na_{0.60}VO_2$ (Average Structure)

P′3-Na_xVO_2	d (Å)	P′3-Na_xVO_2	d (Å)
2*V1−O1	1.96(2)	2*O1−O1	2.61(2)
4*V1−O1	1.926(14)	1* Na1−O1	2.37(4)
2*O1−O1	2.870(8)	2*Na1−O1	2.56(4)
4*O1−O1	2.88(3)	1* Na1−O1	2.30(5)
1*O1−O1	2.57(3)	2* Na1−O1	2.64(3)
2*V1−V1	2.871	4*V1−V1	2.877

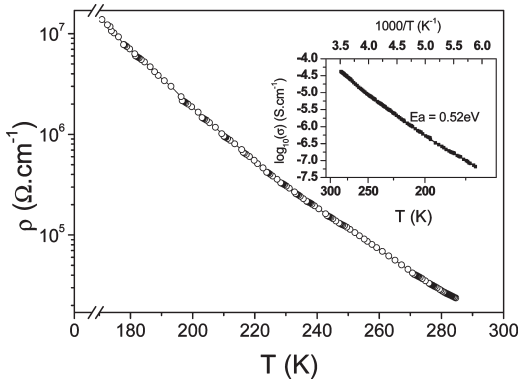

Figure 7. Temperature dependence of the electrical resistivity measured on sintered pellets for P′3-$Na_{0.60}VO_2$ between 170 and 300 K. The inset represents an Arrhenius plot of the conductivity versus reciprocal temperature. The activation energy has been deduced from the slope of the curve and is equal to 0.52 eV.

Conductivity. Figure 7 shows the electrical resistivity ρ of a P′3-$Na_{0.60}VO_2$ pellet from 170 to 300 K. The temperature dependence is semiconductor-like with a resistivity on the order of 10^4 Ω·cm at room temperature when in the homologous phase P′3-$Na_{0.50}CoO_2$;[21] the electrical resistivity is equal to 10^{-2} Ω·cm at 298 K. In the

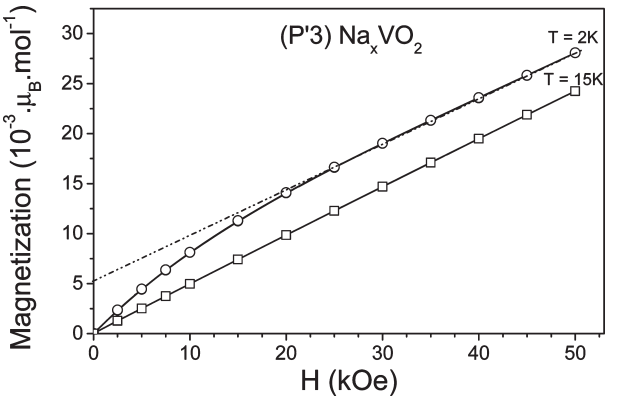

Figure 8. Applied field dependence of the magnetization curve of P′3-$Na_{0.60}VO_2$ at $T = 2$ and 15 K.

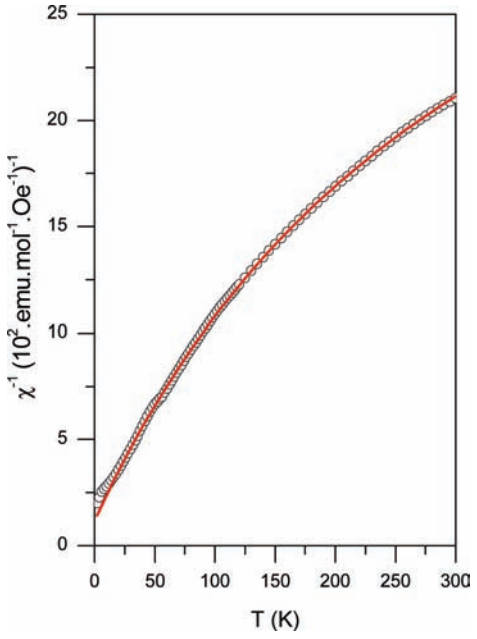

Figure 9. Reciprocal magnetic susceptibility of P′3-$Na_{0.60}VO_2$ versus T for $H = 5$ kOe. The susceptibility has been measured in a 2 K < T < 300 K range. The red line represents the fit of the data with a Curie−Weis law, with the refined parameters $C = 0.0761(4)$ emu·K^{-1}·mol^{-1}·Oe^{-1}, $\theta_p = -9.0(3)$ K, and with a van Vleck contribution.

whole temperature range, an activation energy of $E_a = 0.52$ eV has been calculated (inset in Figure 7) using an Arrhenius plot where $\rho \propto \exp(E_a/T)$. One can conclude that the electrons are strongly localized in $Na_{0.60}VO_2$.

Magnetic Properties and Specific Heat. The variations of the magnetization versus the applied magnetic field for $T = 2$ and 15 K are shown in Figure 8. It can be noticed that the variation at $T = 2$ K is slightly curved, while at $T = 15$ K, it becomes clearly linear (Figure 8). It has also been found that there is no hysteresis between the zero-field-cooled and field-cooled processes.

Thermal variation of the reciprocal susceptibility of $Na_{0.60}VO_2$ at $H = 5$ kOe is given in Figure 9. The small kink observed below $T < 15$ K can be explained by the H dependence of the magnetization in this temperature range (Figure 8). The very small kink observed at $T \approx 50$ K is due to the signal of oxygen traces in the SQUID magnetometer. Two observations can be done: the first one is that the magnetic susceptibility does not exhibit any

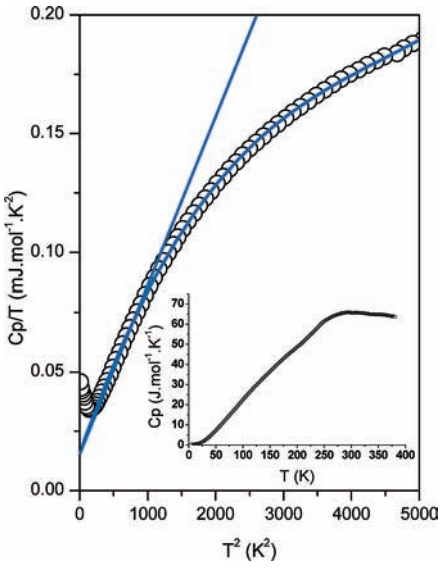

Figure 10. T^2 dependence of Cp/T of P′3-$Na_{0.60}VO_2$ measured between 2 and 200 K. The inset represents the heat capacity versus T. The straight blue line represents the first-order fit of the data with the equation $Cp/T = \gamma + \beta_3T^2 + \beta_5T^4 + \beta_7T^6$, and the curved blue line represents the third-order fit of the data. All refined parameters are gathered in Table 4.

magnetic transition down to $T = 2$ K. This result has been confirmed by measurement of the specific heat down to $T = 2$ K (Figure 10), where no λ-type peak characteristic of a long-range magnetic ordering is observed. The second observation is that, in the whole temperature range, $Na_{0.60}VO_2$ behaves as a paramagnetic phase. However, the susceptibility values, especially at low temperatures ($T = 4$ K, $\chi = 0.00387$ emu·mol^{-1}·Oe^{-1}), are very small compared to those of an ideal paramagnetic phase. This is the signature of the existence of strong antiferromagnetic exchange interaction within the vanadium lattice. In the whole range of temperature, the magnetic susceptibility apparently follows a Curie−Weiss law $\chi = C/(T - \theta_p) + \chi_0$, with $C = 0.076(4)$ emu·K^{-1}·mol^{-1}·Oe^{-1}, $\theta_p = -9.0(3)$ K, and $\chi_0 = 227(2) \times 10^{-6}$ emu·mol^{-1}·Oe^{-1}. χ_0 corresponds to the van Vleck orbital and diamagnetic components.

The Curie constant obtained is significantly smaller than the one expected from a pure ionic state of xV^{3+} ($S = 1$) and $(1 - x)V^{4+}$ ($S = {}^1/_2$) for the formula Na_xVO_2 with $x = 0.60$. Indeed, assuming a g factor = 2 for the two ions and also a spin-only contribution, one should expect a Curie constant close to $C = 0.75$ emu^{-1}·K^{-1}·mol^{-1}·Oe^{-1}. A similar result has been observed for $Na_{0.70}VO_2$, which corresponds to a P2 phase where the oxygen stacking is a AABB sequence.[24] The magnetic susceptibility of P2-$Na_{0.70}VO_2$ at low temperatures follows also a Curie−Weiss law type with $C = 0.08(1)$ emu·K^{-1}·mol^{-1}·Oe^{-1}, $\theta_p = -16.6$ K, and $\chi_0 = 40 \times 10^{-6}$ emu·mol^{-1}·Oe^{-1}. In ref 24, an explanation of the thermal dependence of the susceptibility has been given based on a pseudotrimer model, where the V−V antiferromagnetic exchange interaction is expressed on the basis of a Heisenberg−Dirac model. In an ideal triangular lattice, the frustrating geometry prevents all nearest-neighbor antiferromagnetic interactions from being satisfied simultaneously. The ground state is degenerate, and consequently these systems undergo structural distortions at low temperatures, with a lowering

of the symmetry implying a suppression of the degeneracy. An orbital ordering mechanism has been suggested by which the geometric frustration can be removed to lower the energy of the system.[26,34−36] If one follows the local triangular cluster approach, one can estimate the Curie constant for $T \ll J/k$, where J/k is the V−V intratrimer exchange interaction constant. In the P2-$Na_{0.70}VO_2$ phase, the energy gap between the ground state and the first excited state has been estimated as $\Delta E \approx 350$ K. The similarities of the magnetic susceptibilities of P2-$Na_{0.7}VO_2$ and P′3-$Na_{0.60}VO_2$ at low temperatures lead to the conclusion that the Curie constant observed in this temperature range is mainly governed by the spin multiplicity of the ground state. Compared to $NaVO_2$, in which only one type of triangular spin configuration has to be considered (for $x < 1$ in the Na_xVO_2 formula), one has to consider four types of local triangular spin configuration clusters weighted by a random distribution varying with the x value. On the basis of the Heisenberg−Dirac model, the spin Hamiltonian of a triangular trimer can be expressed as $H = -2J(\mathbf{S}_1\cdot\mathbf{S}_2 + \mathbf{S}_2\cdot\mathbf{S}_3 + \mathbf{S}_1\cdot\mathbf{S}_3)$, where J is the isotropic V−V exchange interaction constant, $\mathbf{S}_{1\rightarrow3}$ is the spin operator associated with the spin value $S_{1\rightarrow3}$. The eigenvalue of the Hamiltonian, which corresponds to the energy level of the cluster, can easily be calculated using a vectorial decomposition of the total spin S_t of the trimer where $S_t = S_1 + S_2 + S_3$. The general expression of the energy levels is

$$E_{S_t} = -J[S_t(S_t + 1) - \sum_{i=1}^{3} S_i(S_i + 1)]$$

(i) The first type of spin configuration to be considered corresponds to three V^{3+} ions with $S_i = 1$. The calculation shows that the ground state is a singlet with $S_t = 0$. The energy gap with the first exited state is $\Delta E = |2J|$.

(ii) The second type of spin configuration corresponds to three V^{4+} ions with $S_i = {}^1/_2$. In this case, the energy diagram is characterized by a doublet ground state with $S_t = {}^1/_2$. The energy gap with the spin state $S_t = {}^3/_2$ is equal to $\Delta E = |3J|$.

(iii) The third type of trimer corresponds to the spin configuration of two spins $S_i = {}^1/_2$ and one spin $S_i = 1$. In this case, the ground state is nonmagnetic ($S_t = 0$) and the energy gap with $S_t = 1$ is $|2J|$.

(iv) Finally, the fourth type of cluster corresponds to one spin $S_i = {}^1/_2$ and two spins $S_i = 1$. The ground state is a spin doublet with $S_t = {}^1/_2$. The energy gap with $S_t = {}^3/_2$ is $\Delta E = |3J|$.

Considering a random distribution of V^{3+} and V^{4+} ions in the pseudotriangular clusters, one can estimate the C Curie constant. An enumeration of the different combination p^n ($2^3 = 8$) for the formula $Na_xV^{3+}{}_xV^{4+}{}_{1-x}O_2$ was done where n refers to the number of neighbors and p refers to the number of possibilities. The probability of the two trimer configurations having the ground state $S_t = {}^1/_2$ is equal to $(3!/3!0!)(1-x)^3$ [$=(1-x)^3$] and $(3!/2!1!)x^2(1-x)$ [$=3x^2(1-x)$]. The general expression of the Curie constant versus x is $[(1-x)^3 + 3x^2(1-x)]/3 \times 0.375$. The variation of C for $0 < x < 1$ is given in Figure 11. One can observe a large plateau for $0.25 < x < 0.75$. Considering $x = 0.60$, the calculation of the Curie constant leads to $C = 0.062$ emu·K^{-1}·mol^{-1}·Oe^{-1}, which is in good agreement with the observed Curie constant $C = 0.076$ emu·K^{-1}·mol^{-1}·Oe^{-1} deduced from the magnetic susceptibility. One can notice that, for $x = 0.7$, the calculated value = 0.059 emu·K^{-1}·mol^{-1}·Oe^{-1} is close to the one reported by Onoda, $C_{exp} = 0.080$ emu·K^{-1}·mol^{-1}·Oe^{-1}. Two observations can be done. First, the two experimental Curie constants are very close ($C_{exp} \approx 0.08$ emu·mol^{-1}·K^{-1}), as predicted by our calculation ($C_{calc} \approx 0.06$ emu·mol^{-1}·K^{-1}). Second, in our theoretical model, the V^{3+} and V^{4+} g factors are assumed to be the same and equal to 2; this could explain the discrepancy between the experimental and calculated values.

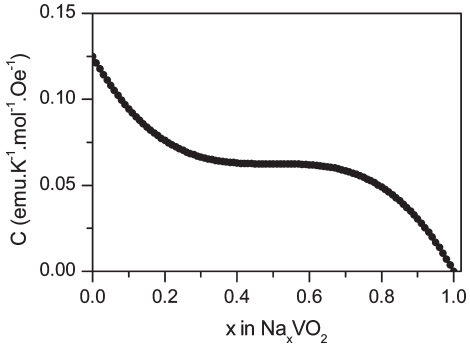

Figure 11. x value dependence of the theoretical C Curie constant by assuming a pseudotriangular cluster model where x is the composition in $Na_xV^{3+}{}_xV^{4+}{}_{1-x}O_2$. The C Curie constant is calculated on the basis of the ground state of the total spin $S_t = {}^1/_2$: $C_{th} = [(1-x)^3 + 3x^2(1-x)]/3 \times 0.375$.

Figure 10 represents the temperature dependence of the specific heat of P′3-$Na_{0.60}VO_2$. As previously written, no transition peaks are observed, which indicates that no magnetic and/or structural transition happened in the T range analyzed. Below $T = 12$ K, the Cp/T plot exhibits a Schottky anomaly, which could be explained by the presence of either strong spin/electron correlations or impurities. To determine the Sommerfeld ratio γ and the Debye temperature, the first-order (limited to T^2) part of $Cp/T = \gamma + \beta_3T^2 + \beta_5T^4 + \beta_7T^6$ was fitted (Figure 10 and Table 4). The value of $\gamma = 20.4$ mJ·mol^{-1}·K^{-2} is higher than that for a metal such as copper (≈6 mJ·mol^{-1}·K^{-2}),[37] which is a signature of strong spin/electron correlations. The β_3 coefficient allows us to evaluate a Debye temperature of 312 K ($\beta_3 = 12\pi^4R/5\theta_D{}^3$). The result of the fit shows that Cp/T is not strictly linear with T^2 and that the highest temperature terms (up to T^6) are necessary to well define the high-temperature behavior (Figure 10 and Table 4). One can notice that γ and β_3 change only slightly with the limitation of the fit. The second observation is that the β_5 and

(34) Onoda, M.; Nagasawa, H. *Butsuri* (*Bull. Phys. Soc. Jpn.*) **1994**, *49*, 559 (in Japanese).
(35) Naka, T.; Onoda, M.; Nagasawa, H. *Solid State Commun.* **1993**, *87*, 679.
(36) Pen, H. F.; van den Brink, J.; Khomskii, D. I.; Sawatzky, G. A. *Phys. Rev. Lett.* **1997**, *78*, 1323.
(37) Mahan, G. D. In *Solid State Physics*; Ehrenreichand, H., Spaepen, F., Eds.; Academic Press: New York, 1998; Vol. *51*, p 81.

Table 4. Parameters Obtained from the Fit of the Specific Heat of $Na_{0.60}VO_2$ (This Work) Using (*) the Equation $Cp/T = \gamma + \beta_3 T^2$ and (**) the Equation $Cp/T = \gamma + \beta_3 T^2 + \beta_5 T^4 + \beta_7 T^6$ and (***) from the Fit of the Specific Heat of $Na_{0.55}CoO_2$[38]

composition	γ (mJ·mol^{-1}·K^{-2})	β_3 (mJ·mol^{-1}·K^{-4})	β_5 (mJ·mol^{-1}·K^{-6})	β_7 (mJ·mol^{-1}·K$^{-8)}$	θ_D (K)
$Na_{0.60}VO_2$*	20.4(1)	$60.0(4) \times 10^{-3}$			312
$Na_{0.60}VO_2$**	19.6(5)	$74.4(7) \times 10^{-3}$	$-117(1) \times 10^{-6}$	$7.0(3) \times 10^{-10}$	296
$Na_{0.55}CoO_2$[38]***	54.0(2)	268×10^{-3}	-195×10^{-6}	131×10^{-10}	372

β_7 values are comparable to the ones reported for $Na_{0.55}CoO_2$[38] (Table 4).

Conclusion

A new compound P′3-$Na_{0.60}VO_2$ has been synthesized by means of a soft chemistry route. The $Na_{0.60}VO_2$ compound exhibits a monoclinic distortion (P′3) in relation to the AABBCC stacking (P3) with the unit cell parameters a = 4.9862(14) Å, b = 2.8708(8) Å, c = 5.917(2) Å, and β = 104.36(3)°. A modulated structure was observed by TEM and XRD measurements. The XRD pattern was fully indexed by a 4D approach taking into account the superspace group $C2/m$ (0 β 0) s0 and a **q** vector equal to 0.44***b****. The physical characterizations indicate that the compound presents a strong correlated system. These correlations could be explained by a pseudotriangular cluster model. Further studies of the solid solution Na_xVO_2 around the composition $Na_{0.60}VO_2$ are in progress to check if a relationship between the components of the **q** vector and the composition exists. Growing single crystals will be helpful to determine structures using the superspace formalism.

Acknowledgment. The authors thank C. Denage for her technical assistance and R. Decourt for the specific heat experiments.

(38) Ando, Y.; Miyamoto, N.; Segawa, K.; Kawata, T.; Terasaki, I. *Phys. Rev. B* **1999**, *60*, 10580.